J MATER SCI **41** (2006) 2605–2610

Cube-phase in excess Mg-type Al–Mg–Si alloy studied by EFTEM

KENJI MATSUDA*, YOSHITAKA ISHIDA
Faculty of Engineering, Toyama University, Toyama, 930-8555, Japan
E-mail: matsuda@eng.toyama-u.ac.jp

I. MULLEROVA, L. FRANK
Institute of Scientific Instruments, Academy of Sciences of Czech Republic, Brno, Czech Republic

SUSUMU IKENO
Faculty of Engineering, Toyama University, Toyama, 930-8555, Japan

Published online: 17 April 2006

The cube-shaped phase (cube-phase) in an aged Al–Mg–Si alloy including Mg in excess has been investigated by an energy-filtering transmission electron microscope (EFTEM) equipped with an energy dispersive X-ray spectrometer (EDS) to determine its chemical composition. The quantitative chemical compositions of cube-phase and β-phase (Mg_2Si) were determined from EELS elemental maps. These data were also in good agreement with their EDS data. The cube-phase contained higher Mg content than the equilibrium β-phase (Mg_2Si), although they had the same crystal lattice of fcc, as reported by some previous researchers.

1. Introduction

In addition to the equilibrium β-Mg_2Si phase, a cube-shaped phase has been also reported in a quasi-binary Al-Mg_2Si alloy as well as excess Mg-type alloys by some researchers and it has been discussed whether it is the precursor of the β-phase or not [1–3]. Its chemical composition, however, has not been well investigated yet. Recently energy-filtering transmission electron microscopy (EFTEM) for quantitative chemical composition has been applied to precipitates in aluminium alloys by the present authors, and it has been demonstrated that this technique is a very powerful tool for the determination of the chemical composition in nano-regions [4, 5]. In this work, the cube-shaped phase in a quasi-binary Al-Mg_2Si alloy as well as an alloy with Mg in excess has been investigated by EFTEM and energy dispersive spectroscopy (EDS) in order to determine its crystal structure and its chemical composition. Furthermore, the quantitative chemical composition has been calculated using the intensity of EELS elemental maps obtained from the cube-phase.

2. Experimental procedures

2.1. Alloys and heat treatment

An Al −1.0 mass% Mg_2Si quasi-binary alloy (balanced alloy) and an Al −1.0 mass% Mg_2Si −0.4 mass% Mg alloy (excess Mg alloy) used in the present study were prepared by a conventional ingot metallurgy using 99.99 mass% purity Al and 99.9 mass% Mg and 99.9 mass% Si ingots. Impurities, such as Fe, Cr, or Cu, were less than 0.02 mass%. These ingots were hot-and cold-rolled to 0.2-mm thick sheets. These sheets were solution heat-treated at 848 K for 3.6 ks and then quenched into chilled water at 277 K. The aging treatment was performed in a salt bath at 673 K for the balanced alloy, and at 623 K for the excess Mg alloy.

2.2. TEM observation

Thin foils for TEM observation were prepared by a conventional electro-polishing method using a mixture of 10% perchloric acid and 90% ethanol at 253 K. An EFTEM used for the present work was a 400 kV

*Author to whom all correspondence should be addressed.
0022-2461
DOI: 10.1007/s10853-006-7819-6

high-resolution TEM (JEOL 4010T) equipped with a post-column type energy filter (Gatan GIF 200), and EDS (Noran Voyager-4).

Elemental maps for each element were obtained using a Gatan GIF200 by the three-windows method with higher loss electron energies, to reduce the effect of the strain contrast. The equation used for quantifying the chemical composition from elemental mapping intensity was as follows [6],

$$n_A = \frac{I_A}{I_T} \cdot \frac{1}{t \cdot \sigma_A(\beta, \Delta E, E_0)} \quad (1)$$

n_A is the area density of the element. I_A is intensity of elemental mapping per unit time. I_T is zero-loss intensity per unit time. t is thickness. σ_A is a partial cross section for energy losses within a range Δ of the ionization threshold and for scattering angles up to β. This calculation can be done by EL/P software of Gatan.

3. Results

3.1. Application of EFTEM method to the β-phase

Fig. 1 shows the microstructure of the balanced alloy aged at 673 K for 1.8 ks. The particular grain of the Al matrix shown in Fig. 1b was nearly parallel to [001] direction, and many square-shaped precipitates can be seen. This is a typical β-Mg_2Si phase. The β-Mg_2Si is a platelet, having the following crystallographic orientation relationship with the Al-matrix [1, 2, 5]:

$$\{001\}_\beta // \{001\}_{Al}, \quad \langle 100\rangle_\beta // \langle 110\rangle_{Al}$$

Elemental maps of Mg and Si were obtained from the β-Mg_2Si phase shown in Fig. 2. As this β-Mg_2Si phase is end-on, its plane surface is perpendicular to the TEM foil and parallel to the viewing direction. Its original depth should be the same as its width, 200 nm longer than its thickness of 40 nm. Since the thickness of the Al-matrix was 98 nm as determined by EELS, neither the

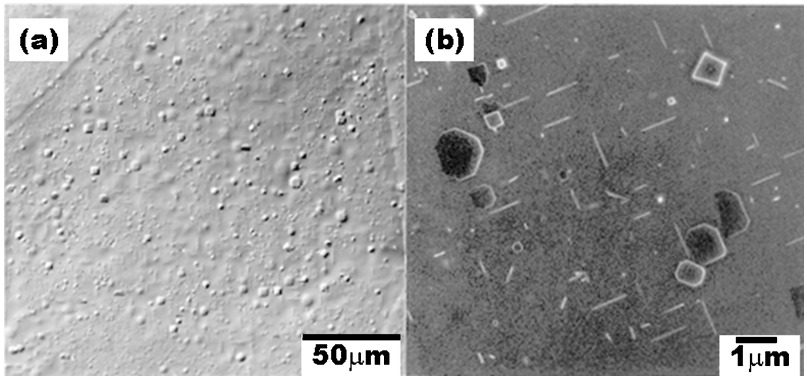

Figure 1 Microstructure of the β-Mg_2Si phase in the balanced alloy aged at 673 K for 1.8 ks. (a) Optical and (b) scanning electron micrographs.

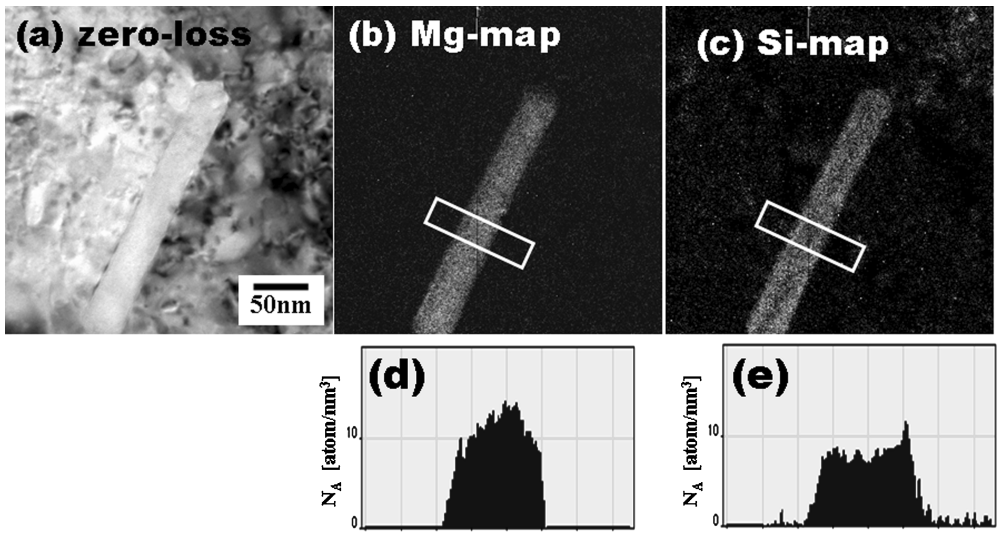

Figure 2 EFTEM images obtained from the β-Mg_2Si phase in the balanced alloy aged at 673 K for 1.8 ks. (a) zero-loss image, (b) Mg-K and (c) Si-K maps. (d) and (e) are the results of quantitative analysis of Mg and Si maps.

top nor the bottom surface of β-Mg_2Si phase was covered by the matrix. This is good to detect elemental maps. Quantitative chemical compositions were calculated from intensities of Figs. 2b and c using Equation 1, and their results were shown in Figs. 2d and e. As the average numbers of Mg and Si atoms per unit volume in this phase are 31.2 and 15.6 atom/nm^3 respectively, the ratio of Mg/Si is about 2. This result is quite good as a reference for determination of the chemistry of an unknown precipitate. The EDS spectrum was not shown here, but the ratio of Mg/Si obtained from the β-Mg_2Si phase was about 2. This result also supports a result of chemical composition calculated from the elemental maps by EELS.

3.2. Application of EFTEM method to the cube-phase

Fig. 3 shows low-magnification TEM images obtained on the excess Mg alloy aged at 623 K for 6 ks. The square- and rectangular-shaped precipitates were visible in the dark-field image shown in Fig. 3b. As the square-shaped ones are the target of the present work, the rectangular ones will not be mentioned hereafter. The sides of these square-shaped ones were parallel to the [100] and [010] directions of the Al matrix. This is a typical cube-shaped phase [1–3], and is referred to as the cube-phase in the present study. The corresponding selected area diffraction pattern from this cube-phase precipitate is shown in Fig. 4. It can be indexed as an fcc crystal lattice with $a = 0.633$ nm,

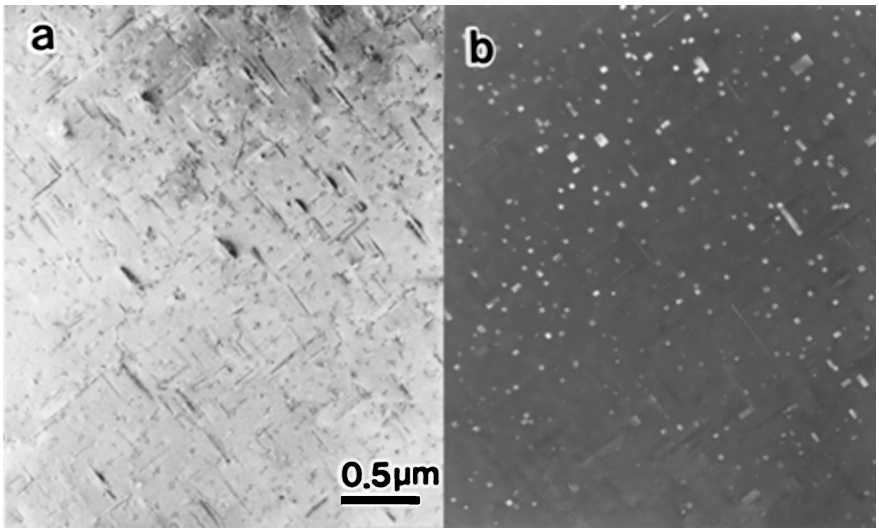

Figure 3 TEM images obtained from the excess Mg alloy aged at 623 K for 6 ks. (a) bright-field and (b) dark-field images.

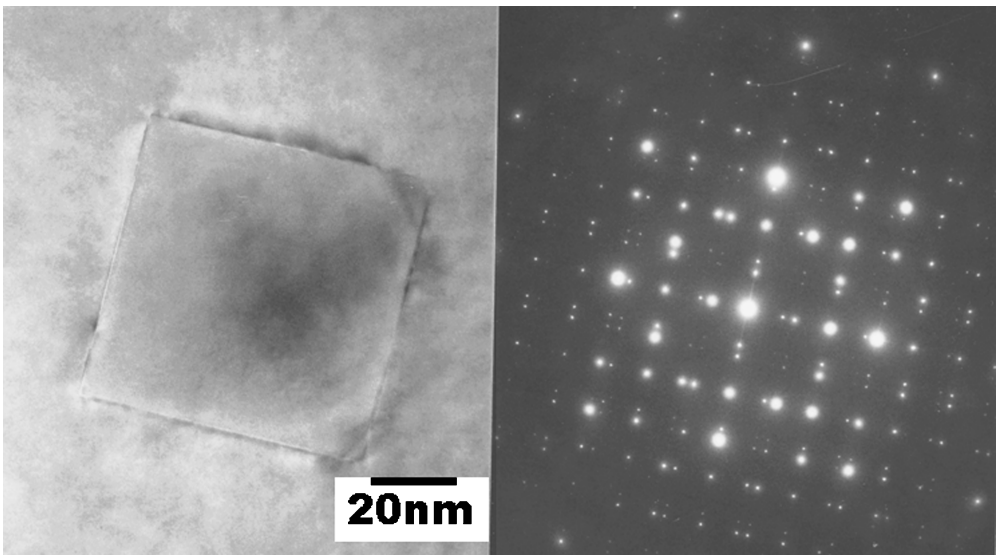

Figure 4 TEM images obtained from the excess Mg alloy aged at 623 K for 6 ks. (a) bright-field image and (b) its selected-area diffraction pattern.

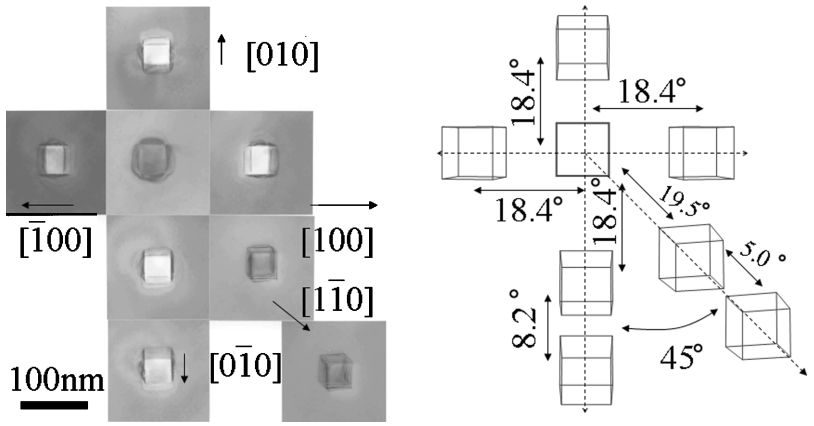

Figure 5 Confirmation of the morphology of the cube-phase by *in situ* tilting. (a) actual TEM images and (b) their calculated images.

which is the same as that reported by previous researchers [1, 2].

Its shape was also confirmed by tilting the cube-phase in the TEM. The cube-phase was tilted along to ⟨010⟩, ⟨100⟩ and ⟨110⟩ directions of the Kikuchi-line and the change in its shape with tilting was recorded in Fig. 5a. Fig. 5b illustrates the calculated shapes of a cuboid for each tilting angle. As they are in good agreement with each other, this square-shaped one is indeed a cuboid.

EDS analysis was also performed to obtain the chemical composition of the cube-phase. To exclude the effect of the Al-matrix, Mg and Si contents were plotted as a function of Al-content as shown in Fig. 6. By extrapolating the lines of Mg and Si to the intersection of the Y-axis, contents of Mg and Si in the absence of the effect of Al-matrix were determined to be 76.8 and 23.2, respectively. It is noted that the ratio of Mg/Si is not 2:1, but nearly 3:1.

Fig. 7 shows a typical EELS profile detected on a typical cube-phase shown in Fig. 8a. Mg-K and Al-K edges are visible, but Si-K edge of 1839 eV is weak because of the effect of the higher Al-K edge. The thickness of

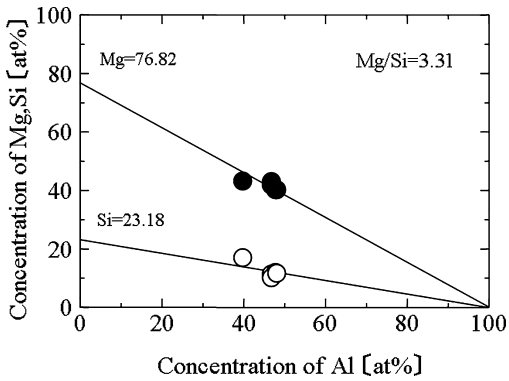

Figure 6 Result of EDS analysis obtained from the cube-phase in the excess Mg alloy aged at 623 K for 6 ks.

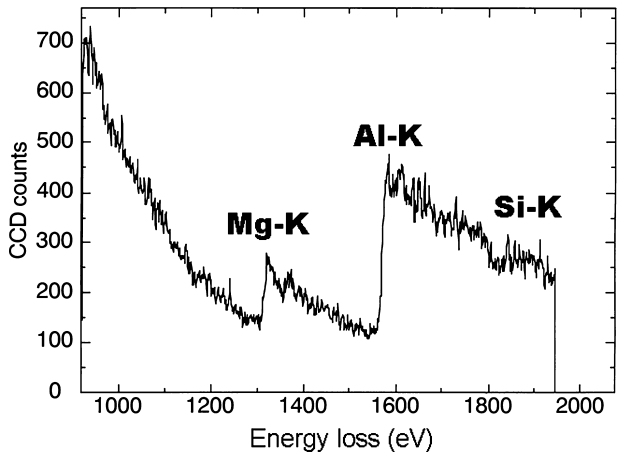

Figure 7 EELS profile obtained from the cube-phase in the excess Mg alloy aged at 623 K for 6 ks.

the matrix calculated by EELS was about 90 nm in this case. As this cube-phase is 60 nm in diameter as shown in Fig. 8a, the Al-matrix, 30 nm thickness altogether, should exist on and/or under this cube-phase. This means that an elemental map obtained using higher energy-loss electrons than the Al-K edge could be weaker than that obtained using energy-loss electrons lower than the Al-K edge. Figs. 8b and c show the Mg-K map (1305 eV) and the Si-K map (1839 eV), respectively. These maps show a bright contrast and they correspond to the precipitate area in a zero-loss image of Fig. 8a. This result supports the assumption described above in that the Si-K map was actually weaker than the Mg-K map.

By using Equation 1, a quantitative chemical composition of this cube-phase was calculated from these elemental maps. The quantitative results of Mg and Si were illustrated in Figs. 8d and e which were obtained from areas marked by white rectangles in Figs. 8b and c. The average value of Mg and Si were 38.0 and 12.3 atom/nm^3, and the ratio of Mg/Si was 3.09, which is almost the same as the EDS analysis shown in Fig. 6.

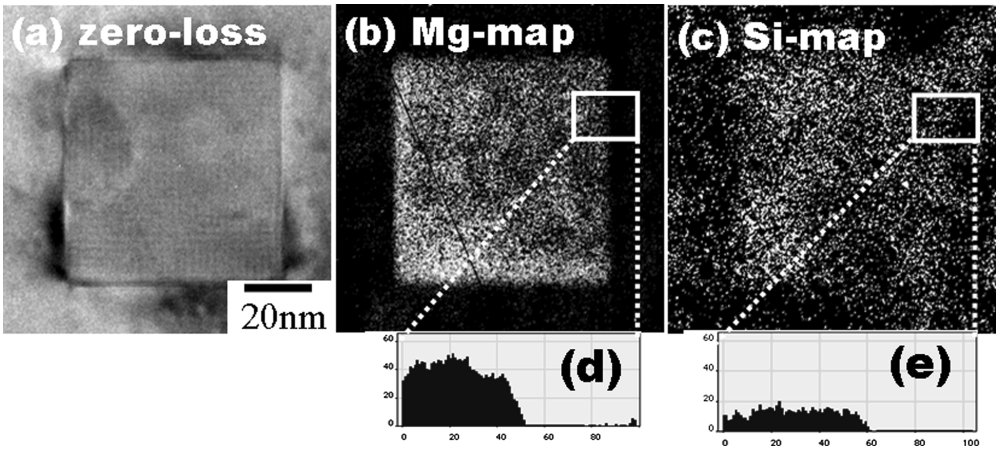

Figure 8 EFTEM images obtained from the cube-phase in the excess Mg alloy aged at 623 K for 6 ks. (a) zero-loss image, (b) Mg-K and (c) Si-K maps. (d) and (e) are the results of quantitative analysis of Mg and Si maps.

4. Discussion

According to EFTEM and EDS analyses, the cube-phase is not Mg_2Si, but probably Mg_3Si. Westengen and Ryum reported the cube-phase as an equilibrium β-Mg_2Si phase but with a different shape and orientation relationship. Kanno and Suzuki *et al*. [2, 7] concluded that the cube-phase is an intermediate phase between the rod-shaped β'-phase and the plate-shaped β-Mg_2Si phase, and that plays an important role in precipitation of the β-Mg_2Si phase. Ohmori *et al*. [3] reported that cube-phase has the same crystal structure as the plate-shaped β-Mg_2Si phase, but with different orientation relationships. In the present work, it was shown that the cube-phase contained a higher Mg content than β-Mg_2Si phase. As the cube-phase is an intermediate phase between the β'-phase and β-Mg_2Si [7], and the crystal lattice of β-Mg_2Si is similar to that of the cube-phase [3], there is a possibility that the cube-phase has a non-stoichiometric composition of β-Mg_2Si with Si atoms replaced by Mg atoms. This assumption maybe supported by the fact that the atomic radii of Mg and Si are similar to each other.

It has been also pointed out that a precipitation of the cube-phase depends on the concentration of the quenched-in vacancies [1–3]. In general, it is known that the precipitation sequence of this alloy system is as follows:

$$\text{Cluster} \rightarrow \text{G.P. zone} \rightarrow \beta'\text{-phase} \rightarrow \beta'\text{-phase} \rightarrow \beta\text{-}Mg_2Si.$$

The clusters or G. P. zones, which consist of Mg, Si and vacancies (Mg-Si-V), are the beginning of precipitation, and vacancies plays an important role in nucleation [8, 9]. The excess Mg alloy contains a higher Mg content and much more numerus clusters of Mg-vacancies can be formed than the balanced alloy in addition to normal Mg-Si-V clusters. As the binding energy of Mg and a vacancy (Mg-V) is lower than that of Si and a vacancy (Si-V) [10], the Mg-V cluster can be formed more easily than a Si-V cluster in the excess Mg alloy. Diffusion and migration energies of Mg in Al, however, are higher than those of Si in Al [11–13]. Thus, Mg atoms can be trapped around the nucleation site, if there are enough Mg atoms in the matrix in the case of the excess Mg alloy. As the diffusion of Si is easier and faster than Mg, this Mg-V cluster will grow into the cube-phase by diffusion of Si from the matrix, or given heterogeneous nucleation site for the cube-phase directly. The nucleation and growth of the cube-phase should be investigated in future studies to clarify the formation mechanisms of this phase.

5. Conclusion

The quantitative analysis by EFTEM was applied to the determination of the β-Mg_2Si phase in the balanced alloy and cube-shaped phase in excess Mg alloy. An extrapolation method for the quantitative analysis by EFTEM of nano-scaled precipitates in Al alloys in the presence the effect of the Al-matrix was developed. The quantitative chemical composition of plate-shaped β-phase was calculated from its elemental map and it was equal to the equilibrium Mg_2Si. On other hand, the cube-phase included higher Mg content than β-Mg_2Si phase.

Acknowledgment

This work was completed as a part of the research project on 'Development of the new lightweight materials by controlling of nano-structure' in the Venture Business Laboratory of Toyama University.

References

1. H. WESTENGEN and N. RYUM, *Z. Metallkde* **70** (1979) 528.
2. M. KANNO, H. SUZUKI and Y. SHIRAISHI, *J. Japan Inst. Metals* **43** (1979) 81.

3. Y. OHMORI, L. C. DOMAN, Y. MATSUURA, S. KOBAYASHI and K. NAKAI, *Mater. Trans.* **42** (2001) 2567.
4. K. MATSUDA, D. TEGURI, Y. UETANI, T. SATO and S. IKENO, *Scripta Mater.* **47** (2002) 833.
5. K. MATSUDA, T. KAWABATA, Y. UETANI, T. SATO and S. IKENO, *J. Mater. Sci.* **37** (2002) 3369.
6. R. F. EGERTON, "Electron Energy-Loss Spectroscopy in Electron Microscopy", 2nd edition (Plenum Press, New York, 1996).
7. H. SUZUKI, M. KANNO and G. ITO, *J. Japan Inst. Light Metals* **32** (1982) 290.
8. I. DUTTA and S. M. ALLEN, *J. Mater. Sci. Letter* **10** (1991) 323.
9. J. D. BRYANT, *Metall. Mater. Trans. A* **30A** (1999) 1999.
10. N. PRABHU and J. M. HOWE, *Metall. Trans. A* **23A** (1992) 135.
11. W. D. CALLISTER JR., "Materials Science and Engineering", 2nd edition, (John Wiley & Sons, Inc., 1991) p. 105.
12. "Kinzoku data book", in Japanese, (Japan Inst. Metals, Japan, 1994), p. 20.
13. N. K. GOBRAN, F. M. MANSY and S. S. HAMZA, *Phys. Stat. Sol. (a)* **59** (1989) 69.